

Dysprosium scandate thin films as an alternate amorphous gate oxide prepared by metal-organic chemical vapor deposition

Reji Thomas,^{a)} Peter Ehrhart, Martina Luysberg, Markus Boese, and Rainer Waser
*Center of Nanoelectronic Systems for Information Technology, Institute for Solid State Research,
 Research Center Juelich, D-52425 Juelich, Germany*

Martin Roeckerath, Eduard Rije, and Juergen Schubert
*Center of Nanoelectronic Systems for Information Technology, Institute of Bio and Nanosystems,
 Research Center Juelich, D-52425 Juelich, Germany*

Sven Van Elshocht and Matty Caymax
IMEC, Kapeldreef 75, B-3001 Leuven, Belgium

(Received 20 July 2006; accepted 16 October 2006; published online 5 December 2006)

Dysprosium scandate (DyScO_3) thin films were deposited on Si substrates using metal-organic chemical vapor deposition. Individual source precursors of Dy and Sc were used and deposition temperatures ranged from 480 to 700 °C. Films were amorphous with low root mean square roughness (≤ 2 Å) and were stable up to 1050 °C annealing. Electrical characterization yielded C-V curves with negligible hysteresis (< 10 mV), high dielectric constant (~ 22), and low leakage currents. The electrical properties of the $\text{DyScO}_3/\text{SiO}_x/\text{Si}$ stacks were stable up to 800 °C for films on native oxide; however, this limit increased to 900 °C for films on special chemically grown oxide, suggesting further improvement with proper diffusion barrier. © 2006 American Institute of Physics. [DOI: 10.1063/1.2402121]

Dielectric materials with sufficiently high dielectric constant (high k) are needed as early as 2007 (Ref. 1) to replace SiO_2/SiON in the future complementary metal oxide semiconductor (CMOS) technology with a subnanometer equivalent oxide thickness. Structural invariance of the thin gate oxide layer within CMOS process thermal budget is preserved with SiO_2 ($\epsilon = 3.9$) and now with SiON ($\epsilon = 7.0$). If one considers this as a major criteria the presently favored group IVB oxides, HfO_2 and ZrO_2 , have to be alloyed with high concentrations of Si or Al in order to stabilize the amorphous structure; however, this alloying reduces the dielectric constant (k) to the values of $\epsilon_r \sim 10$ –12 (Ref. 2) for the silicates of Hf and Zr. Hence, this silicate with medium k may facilitate a smooth transition from conventional gate dielectrics to high- k dielectrics ($k > 20$). In order to reach this target another class of dielectrics with even higher dielectric constants and lower leakage currents is needed. Rare-earth based multicomponent oxides in the amorphous state are being considered as the next generation dielectrics after the silicates.³ Reported work on these types of materials mainly concentrated on the pulsed laser deposition/molecular-beam or electron beam deposition and these reports suggest a very high potential for these materials in the semiconductor industry.^{4–7} An approach by atomic layer deposition of YScO_3 and metal-organic chemical vapor deposition (MOCVD) of DyScO_3 films were reported recently.^{8,9} Our present effort was to realize films of the rare-earth scandate, DyScO_3 , using advanced precursors in an industry friendly high throughput MOCVD process.

In this work, DyScO_3 film depositions were carried out in a liquid injection MOCVD reactor (Aixtron 2600G3 which can handle five 6 in. wafers simultaneously equipped with a liquid delivery Trijet vaporizer).¹⁰

Dy(EDMDD)_3 and Sc(EDMDD)_3 precursors (EDMDD = 6-ethyl-2,2-dimethyl-3,5-decane dionato) were supplied by Asahi Denka, Japan, and were dissolved in octane with 0.05M concentration. This precursor solution was injected by a TRIJET system with a flow rate in the micro-liter regime. Film depositions were carried out in the temperature range of 480–700 °C and the reactor pressure was between 2 and 8 mbars. Oxygen and argon were used as an oxidizer and carrier, respectively.

Si (100) substrates with their native oxide were generally used for the deposition and some wafers with a chemically grown SiO_2 (IMEC cleaned¹¹) were also used for comparison. The composition and areal mass density of the films were routinely determined by x-ray fluorescence (XRF) and checked with Rutherford backscattering spectrometry (RBS). X-ray reflectance and ellipsometry measurements were additionally done to obtain the physical thickness and the density of the layers. Surface morphology and microstructure were investigated with atomic force microscopy (AFM), x-ray diffraction (XRD), and high-resolution transmission electron microscopy (HRTEM). Electrical tests of the metal insulator semiconductor (MIS) capacitors were performed with sputter deposited Pt top electrodes, which had undergone a post-deposition forming gas anneal at 450 °C for 20 min.

Stoichiometric films, $\text{Dy/Sc} \sim 1$, could be deposited within the temperature range from 480 to 700 °C. AFM investigations showed a smooth surface morphology of the films, with a rms roughness of ≤ 0.2 nm, which was achieved independent of the film thickness (2–15 nm). Figure 1 shows a cross sectional HRTEM of a 560 °C deposited, ~ 4 nm thick DyScO_3 on SiO_x/Si which had undergone an annealing in nitrogen at 900 and 1000 °C, depicting the amorphous nature of the DyScO_3 film upon high temperature annealing. An interlayer (IL) of $\sim 2 \pm 0.3$ nm thickness was present between the as-deposited amorphous film and Si (100) substrate (TEM not shown), and IL thickness increased

^{a)}Electronic mail: thomas@iwe.rwth-aachen.de

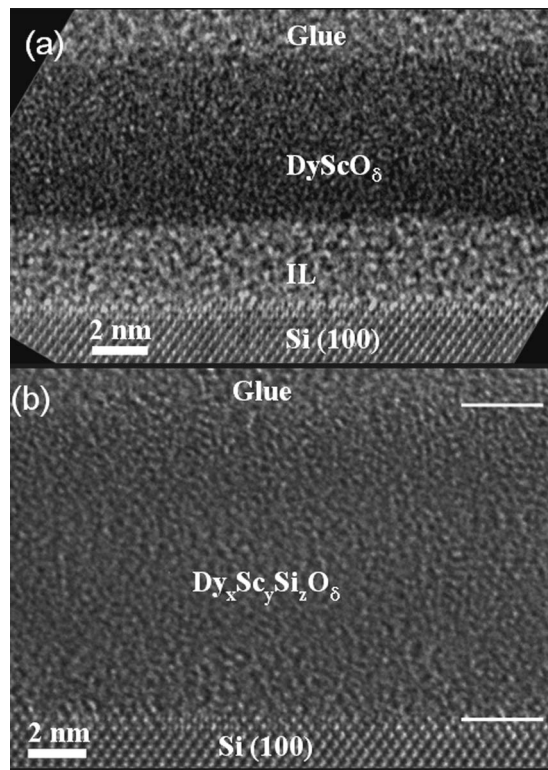


FIG. 1. HRTEM micrograph of a 560 °C deposited, 4 nm thick DyScO_3 film on SiO_x/Si annealed at 900 and 1000 °C; the amorphous structure and interlayer are verified.

to $\sim 2.6 \pm 0.3$ nm upon annealing at 900 °C [Fig. 1(a)]. It is clear from Fig. 1(b) that interdiffusion and stability of this interlayer (SiO_x) are a concern at high temperature, e.g., 1000 °C. Detailed TEM analysis over different regions revealed the disappearance of SiO_x interlayer in most of the regions, but at some regions the interlayer was visible for this 1000 °C annealed sample. This behavior is suggestive of the quality of the native oxide over the wafer surface: region with dense SiO_2 can suppress this diffusion but the region with less dense SiO_x accelerates this interdiffusion. This was verified with the C - V characteristics of films deposited on specially treated Si surfaces (IMEC cleaned^{9,11}), where the reduction in capacitance was not observed after 900 °C annealing (not shown).

XRD established an amorphous structure of the films, Fig. 2. Nevertheless, we observe a broad peak around 30°, which indicates some short range order. Under annealing in purified nitrogen the amorphous structure and the short range order peak are stable up to 1000 °C. At higher temperatures there is indication for phase segregation to binary oxides, especially Dy oxides as reported earlier.⁴ Remarkably, in contrast to N_2 annealing, O_2 annealing at 1050 °C results in the nearly complete disappearance of the broad peak around 30°, which indicates a change of the short range order structure. RBS indicates strong interdiffusion from Si into the DyScO_3 layer and vice versa as well as indiffusion of additional oxygen at a temperature around 1050 °C. This interdiffusion is supported by the observed density changes, which are summarized in the inset (Fig. 2). Up to annealing temperatures of 800 °C we observe no changes in the density, but for $T \sim 950$ °C there is, for both atmospheres, a small decrease in density and a corresponding increase in thickness. Consistent with the XRD larger differences are

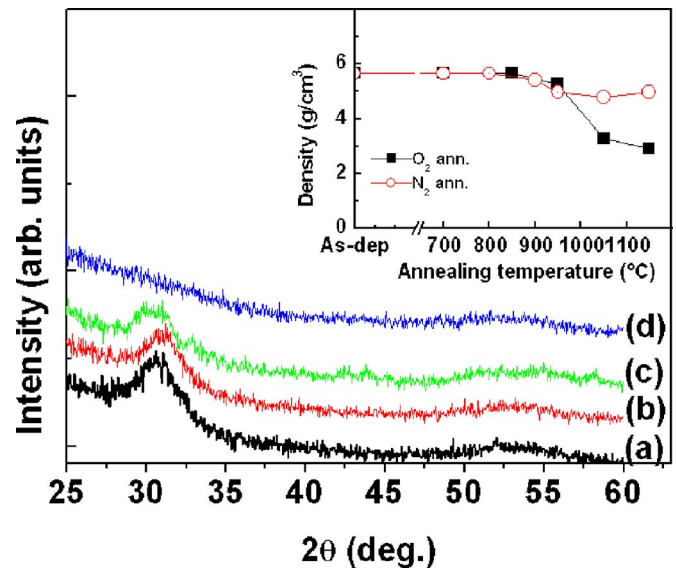


FIG. 2. (Color online) XRD pattern of DyScO_3 films deposited on SiO_x/Si substrates and annealed at various temperatures in nitrogen atmosphere: (a) 800 °C, (b) 900 °C, (c) 1050 °C and oxygen atmosphere, and (d) 1050 °C. The inset shows variation of density as a function of annealing temperature, which is suggestive of strong interdiffusion under O_2 and less significant interdiffusion under N_2 for DyScO_3 films on Si with native oxide.

observed at 1050 °C with much smaller changes under nitrogen atmosphere. In short, stability of the as-deposited film's amorphous structure at a temperature as high as 1050 °C is verified and there is no increase of the surface roughness of the films along with these annealing treatments but interdiffusion is a concern above 800 °C for DyScO_3 films on Si with native oxide.

Electrical properties of MIS capacitors with various thicknesses of DyScO_3 were studied by C - V and I - V characteristics. After an additional postdeposition annealing at 700 °C in N_2 there was no difference for films deposited at different temperatures. C - V curves showed very low hysteresis (< 10 mV) for these films, Fig. 3. Flatband voltage (V_{fb}) was not significantly dependent on the film thickness or equivalent oxide thickness (EOT), and the extracted fixed charge density from the EOT versus V_{fb} plot (inset of Fig. 3)

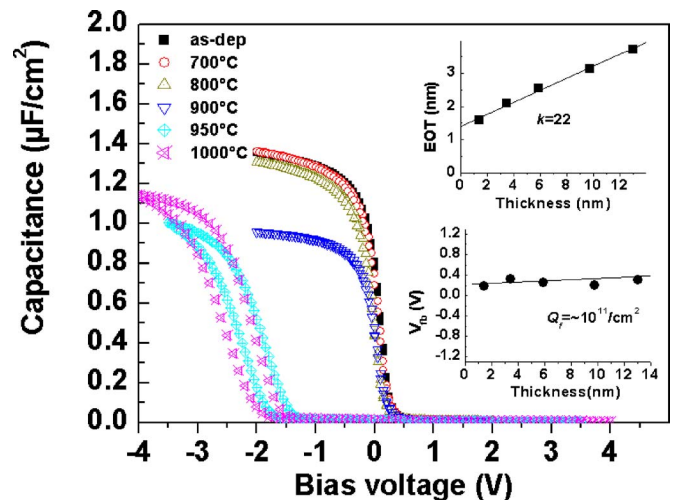


FIG. 3. (Color online) Capacitance-voltage characteristics of the films annealed in N_2 at various temperatures for 20 s. Inset shows EOT and V_{fb} as a function of film thickness; the slope of the EOT fit gives a k value of ≈ 22 and the slope of the V_{fb} fit yields fixed oxide charge density of $\sim 10^{11}/\text{cm}^2$.

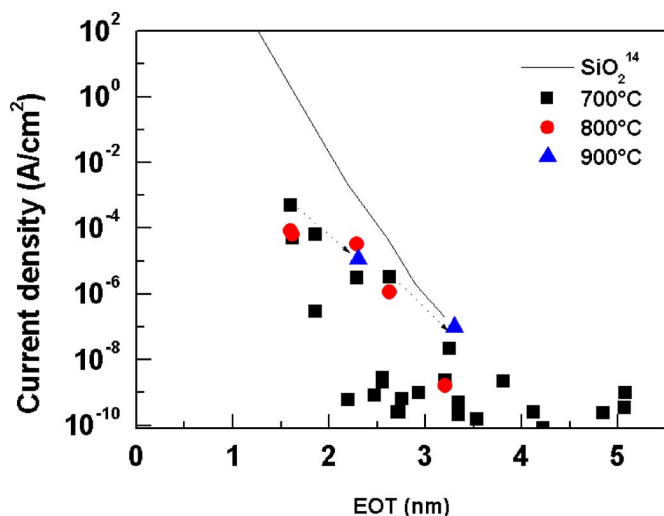


FIG. 4. (Color online) EOT vs current density (at -1 V) for the 700 °C annealed films; annealing at 800 °C shows similar EOT- J values for the same samples, but annealing at 900 °C reduced the leakage current at the cost of EOT.

was $\sim 10^{11}/\text{cm}^2$. From the slope of the linear fit of EOT versus thickness (inset, Fig. 3) a k value of ≈ 22 is derived which is comparable to the best values reported for HfO_2 .^{12,13} The y offset of 1.5 nm corresponds essentially to the nonoptimized interlayer. These promising dielectric data are combined with very low leakage currents (10^{-3} – 10^{-10} A/cm² for film with EOT of 1.5 – 5.5 nm) compared to SiO_2 films, as can be seen from Fig. 4.¹⁴ A direct comparison of leakage current density at $(V_{fb}-1)$ V of this scandate film with the atomic layer deposited HfO_2 films (Ref. 13) having same EOT also shows comparable leakage current even without optimizing the interlayer. In the latter, instantaneous formation of a SiN_x interlayer due to the nitrogen containing precursors prevented the Si diffusion and showed lower EOT and leakage current.¹³ This type of diffusion barrier effect of the IL might be used for DyScO_3 films on Si as well to reduce the leakage current and EOT further.

Annealing studies on the C - V characteristics, Fig. 3, show a reduction in C_{max} at temperatures above 800 °C for films deposited on Si with native oxide due to the interlayer growth and/or interdiffusion. A higher temperature annealing resulted in a very drastic shift in the V_{fb} without much additional reduction in capacitance suggestive of the diffusion of Dy and Sc through the interlayer. This shift in the V_{fb} and the reduction in the C_{max} can be reduced with specially treated Si surface. Our experiment on the IMEC cleaned Si [chemically grown SiO_2 on Si (Ref. 11)] resulted in the same capacitance till 900 °C annealing and the reduction was observed at 1000 °C without much shift in the V_{fb} . This indicates that by optimizing the stability of the interface, interdiffusion can be

suppressed and even higher temperatures might be achievable.

To summarize, stoichiometric DyScO_3 thin films with very smooth surface morphology could be realized with liquid injection MOCVD. Electrical investigation shows very low leakage current densities and C - V curves with negligible hysteresis and low fixed charge density. Dielectric constant was around 22 for this amorphous material and thus it is interesting for scaling down the EOT for ≤ 45 nm node. Although the amorphous structure is retained up to 1050 °C, interdiffusion, which deteriorates the electrical properties, must be considered at temperatures above 800 °C for films on Si with native oxide. Remarkably, this decrease in the capacitance can be delayed till 900 °C by using specially treated Si surface (IMEC clean¹¹). As these reactions depend on the details of the processing, there is much room for optimization, especially considering that the high temperature annealing is performed after electrode deposition, i.e., for a capsulated gate oxide. In addition, these advanced dielectric films will most probably combine with metal gates, which require a different thermal budget. Hence, there is a good chance that the superior properties of this new gate oxide can survive the gate processing.

The authors greatly acknowledge the help of W. Krumpfen for the XRF analysis and H. Haselier for the Pt electrode deposition.

¹International Technology Roadmap for Semiconductors (Semiconductor Industry Association, San Jose, CA, 2005).

²C. M. Osburn, I. Kim, S. K. Han, I. De, K. F. Yee, S. Gannavaram, S. J. Lee, C.-H. Lee, Z. J. Luo, W. Zhu, J. R. Hauser, D.-L. Kwong, G. Lucovsky, T. P. Ma, and M. C. Öztürk, IBM J. Res. Dev. **46**, 299 (2002).

³C. Zhao, T. Witters, B. Brijs, H. Bender, O. Richard, M. Caymax, T. Heeg, J. Schubert, V. V. Afanas'ev, A. Stesmans, and D. G. Schlom, Appl. Phys. Lett. **86**, 132903 (2005).

⁴M. Wagner, T. Heeg, J. Schubert, C. Zhao, O. Richard, M. Caymax, V. V. Afanas'ev, and S. Mantl, Solid-State Electron. **50**, 58 (2006).

⁵T. Heeg, J. Schubert, C. Buchal, E. Cicerella, J. L. Freeout, W. Tian, Y. Jia, and D. G. Schlom, Appl. Phys. A: Mater. Sci. Process. **83**, 103 (2006).

⁶L. F. Edge, D. G. Schlom, P. Sivasubramani, R. M. Wallace, B. Holländer, and J. Schubert, Appl. Phys. Lett. **88**, 112907 (2006).

⁷M. Wagner, T. Heeg, J. Schubert, St. Lenk, S. Mantl, C. Zhao, M. Caymax, and S. De Gendt, Appl. Phys. Lett. **88**, 172901 (2006).

⁸P. Myllymäki, M. Nieminen, J. Niinistö, M. Putkonen, K. Kukli, and L. Niinistö, J. Mater. Chem. **16**, 563 (2006).

⁹S. Van Elshocht, P. Lehen, B. Seitzinger, A. Abrutis, C. Adelman, B. Brijs, M. Caymax, T. Conard, S. De Gendt, A. Franquet, C. Lohe, M. Lukosius, A. Moussa, O. Richard, P. Williams, T. Witters, P. Zimmerman, and M. Heyns, J. Electrochem. Soc. **153**, F219 (2006).

¹⁰P. Ehrhart, F. Fitsilis, S. Regnery, C. Jia, R. Waser, F. Schienle, M. Schumacher, M. Dauelsberg, P. Strzyzewski, and H. Juergensen, Integr. Ferroelectr. **30**, 183 (2000).

¹¹M. M. Heyns, S. Vanhaverbeke, M. Meuris, P. W. Mertens, H. Schmidt, M. Kubota, A. Philiposian, K. Dillenbeck, D. Graf, A. Schneg, and R. De Blank, Mater. Res. Soc. Symp. Proc. **315**, 35 (1993).

¹²A. R. Teren, R. Thomas, J. He, and P. Ehrhart, Thin Solid Films **478**, 206 (2005).

¹³M. Cho, D. S. Jeong, J. Park, H. B. Park, S. W. Lee, T. J. Park, C. S. Hwang, G. H. Jang, and J. Jeong, Appl. Phys. Lett. **85**, 5953 (2004).

¹⁴S.-H. Lo, D. A. Buchanan, and Y. Taur, IBM J. Res. Dev. **43**, 327 (1999).